

# Performance Comparisons of Geographic Routing Protocols in Mobile Ad Hoc Networks

Don Torrieri, *Senior Member, IEEE*, Salvatore Talarico, *Student Member, IEEE*, and Matthew C. Valenti, *Senior Member, IEEE*.

**Abstract**—Geographic routing protocols greatly reduce the requirements of topology storage and provide flexibility in the accommodation of the dynamic behavior of mobile ad hoc networks. This paper presents performance evaluations and comparisons of two geographic routing protocols and the popular AODV protocol. The tradeoffs among the average path reliabilities, average conditional delays, average conditional numbers of hops, and area spectral efficiencies and the effects of various parameters are illustrated for finite ad hoc networks with randomly placed mobiles. This paper uses a dual method of closed-form analysis and simple simulation that is applicable to most routing protocols and provides a much more realistic performance evaluation than has previously been possible. Some features included in the new analysis are shadowing, exclusion and guard zones, distance-dependent fading, and interference correlation.

**Index Terms**—Geographic routing, ad hoc network, area spectral efficiency, path reliability.

## I. INTRODUCTION

MOBILE ad hoc networks often use the *ad-hoc on-demand distance-vector* (AODV) routing protocol [1], which discovers and maintains multihop paths between source mobiles and destination mobiles. However, these paths are susceptible to disruption due to changes in the fading, terrain, and interference, and hence the routing overhead requirements are high. An alternative class of routing protocols that do not maintain established routes between mobiles are the geographic routing protocols. These protocols require only a limited amount of topology storage by mobiles and provide flexibility in the accommodation of the dynamic behavior of ad hoc networks (e.g., [2] - [5] and the many references therein).

Among the many varieties of geographic routing protocols, two representative ones are evaluated in this paper: *greedy forwarding*, which uses beacons, and *maximum progress routing*, which is contention based. The tradeoffs among the average path reliabilities, average conditional delays, average conditional numbers of hops, and area spectral efficiencies and the effects of various parameters are illustrated for finite ad hoc networks with randomly placed mobiles. A comparison

is made with the AODV routing protocol to gain perspective about the advantages and disadvantages of geographic routing.

There has been extensive recent research directed toward providing insights into the tradeoffs among the reliabilities, delays, and throughputs of mobile ad hoc networks with multihop routing (e.g., [6] - [12]). However, the mathematical models and their associated assumptions have not been adequate for obtaining reliable results. Much of this research uses network models based on stochastic geometry (e.g., [13] - [15]) with the spatial distribution of the mobiles following a Poisson point process, and simplifying but unrealistic restrictions and assumptions. One of the principal problems associated with the models based on stochastic geometry is that they assume an infinitely large network with an infinite number of mobiles so that routing in the interior of the network cannot be distinguished from routing that includes a source or destination mobile near the perimeter of the network. The homogeneous Poisson point process does not account for the dependencies in the placement of mobiles, such as the existence of exclusion and guard zones [16] that ensure a minimum spatial separation between mobiles. Typical unrealistic restrictions are the absence of shadowing, the neglect of thermal noise, and the identical fading conditions for each link. Typical unrealistic assumptions are the independence of the success probabilities of paths from the source to the destination even when paths share the same links and the limiting of the number of end-to-end retransmissions rather than link retransmissions. In this paper, all of these unrealistic restrictions and assumptions are eliminated.

In this paper, rigorously derived closed-form expressions of outage probabilities based on the methodology of [19], which we call *deterministic geometry*, are combined with simple and rapid simulations that allow additional network features to be considered. The simulation allows the compilation of statistical characteristics of routing without assumptions about the statistical independence of possible paths. During each simulation trial, the topology is fixed, and we compute outage probabilities and performance measures, and then we average over many topologies. Within each topology, mobiles can be placed according to any distribution, and we focus on uniform clustering with exclusion and guard zones. During each simulation trial, paths for message delivery are selected by using the closed-form expression for the per-link outage probability to determine which paths are possible, and the delay associated with each available link is determined. Using these paths and averaging over many topologies, the dependences of the path reliability, area spectral efficiency, average

Manuscript received Feb. 19, 2015; revised May. 30, 2015; revised Jul. 20, 2015; accepted August 28, 2015. Date of publication XXX. XX, 2015. Date of current version XXX. XX, 2015. The associate editor coordinating the review of this paper and approving it for publication was J. Widmer.

Portions of this paper were presented at the IEEE Military Communications Conference, 2013 and 2014.

D. Torrieri is with the US Army Research Laboratory, Adelphi, MD (email: don.j.torrieri.civ@mail.mil).

S. Talarico and M. C. Valenti are with West Virginia University, Morgantown, WV, U.S.A. (email: salatore.talarico81@gmail.com; valenti@ieee.org).

Digital Object Identifier 15.0162/TCOMM.2015.XX.XXXXXX

message delay, and average number of hops on network parameters such as the source-destination distance, maximum number of transmission attempts per link, and density of mobiles are evaluated. The work presented here is an extension of our preliminary work [17], [18]. For instance, in [17] an earlier form of the methodology is used to analyze three non-geographic routing protocols. In [18], preliminary results for geographic protocols are presented, but they do not account for interference correlation. The present paper provides a deeper analysis by considering the effects of interference correlation, the maximum number of retransmissions, the spreading factor, the contention density, and the relay density.

Among the features of our analysis and simulation that distinguish it from those by other authors are the following:

1. Distinct links do not necessarily experience identically distributed fading. For example, a distance-dependent fading model is adopted in Section IV.
2. Source-destination pairs are not assumed to be stochastically equivalent. For example, if a source or destination is located near the perimeter of the network, the interference and hence the routing characteristics are different from those computed for source-destination pairs near the center of the network.
3. There are no assumptions of independent path selection or path success probabilities. If a link fails, then all potential paths that share that link also fail.
4. The shadowing over the link from one mobile to another can be modeled individually, as required by the local terrain. For computational simplicity in the example network of Section IV, the shadowing is assumed to have a lognormal distribution.
5. The presence of thermal noise, which is integrated into the analysis, is important when the mobile density, and hence the interference, is moderate or low.
6. The routing protocols do not depend on predetermined routes. Instead, they use a more realistic *dynamic route selection* that may include a path-discovery phase using request packets and acknowledgements and a message-delivery phase.
7. Due to the use of an accurate closed-form expression for the outage probability in the presence of fading and interference, the simulation does not need to draw random variables representing the fading and interference conditions.
8. Interference correlation [20], which is an artifact of the fixed positions of the potentially interfering nodes, is naturally taken into account because the topology is fixed for each simulation trial.

The methodology has great generality and can be applied to the performance evaluation of most other routing protocols and types of communication networks and environments within mobile ad hoc networks. By varying the values of several key parameters that are defined in the paper, the essence of many kinds of networks can be captured. Nevertheless, there are some limitations to the approach that arise primarily from fixing the topology. For instance, networks with very high mobility (i.e., if there is significant movement during an end-to-end transmission) or that use store-carry-and-forward protocols cannot be immediately accommodated. However, such networks could be handled through an extension of

the proposed methodology involving the incorporation of a discrete-time mobility model. For ease of exposition, the paper focuses on unicast transmission, but multicast protocols are an obvious extension.

The remainder of this paper is organized as follows. Section II presents the network model, featuring an equation for the outage probability for a link between two mobiles, provides a description of the network simulator, and discusses the issue of interference correlation. Section III describes three routing protocols, the implementation of path selection, and the performance metrics used to evaluate and compare these protocols. In Section IV, numerical results are presented for a typical large network. Finally, the paper concludes in Section V.

## II. NETWORK MODEL AND SIMULATOR

### A. Network Model

The network comprises  $M + 2$  half-duplex mobiles in an arbitrary two- or three-dimensional region. The variable  $X_i$  represents both the  $i^{th}$  mobile and its location, and  $\|X_j - X_i\|$  is the distance from the  $i^{th}$  mobile to the  $j^{th}$  mobile. Mobile  $X_0$  serves as the reference transmitter or message source, and mobile  $X_{M+1}$  serves as the reference receiver or message destination. The other  $M$  mobiles  $X_1, \dots, X_M$  are potentially relays or sources of interference. Each mobile uses a single omnidirectional antenna.

*Exclusion zones* surrounding the mobiles, which ensure a minimum physical separation between two mobiles, have radii set equal to  $r_{ex}$ . The mobiles are uniformly distributed throughout the network area outside the exclusion zones, according to a *uniform clustering* model [16].

The mobiles of the network transmit asynchronous quadrature phase shift keying (QPSK) signals. For such a network, interference is reduced after despreading by the factor  $G/h(\tau_o)$ , where  $G$  is the *processing gain* or *spreading factor*, and  $h(\tau_o)$  is the chip factor [19], which is a function of the chip waveform and the timing offset  $\tau_o$  of the interference spreading sequence relative to that of the desired or reference signal. Since only timing offsets modulo- $T_c$  are relevant,  $0 \leq \tau_o < T_c$ . If  $\tau_o$  is assumed to have a uniform distribution over  $[0, T_c)$  and the chip waveform is rectangular, then the expected value of  $h(\tau_o)$  is  $2/3$ . It is assumed henceforth that  $G/h(\tau_o)$  is a constant equal to  $G/h$  for all mobiles in the network.

Let  $P_i$  denote the received power from  $X_i$  at the reference distance  $d_0$  before despreading when fading and shadowing are absent. After the despreading, the power of  $X_i$ 's signal at the mobile  $X_j$  is

$$\rho_{i,j} = \tilde{P}_i g_{i,j} 10^{\xi_{i,j}/10} f(\|X_j - X_i\|) \quad (1)$$

where  $\tilde{P}_i = P_i$  for the desired signal,  $\tilde{P}_i = hP_i/G$  for an interferer,  $g_{i,j}$  is the power gain due to fading,  $\xi_{i,j}$  is a shadowing factor, and  $f(\cdot)$  is a path-loss function. The path-loss function is expressed as the power law

$$f(d) = \left(\frac{d}{d_0}\right)^{-\alpha}, \quad d \geq d_0 \quad (2)$$

where  $\alpha \geq 2$  is the path-loss exponent, and  $d_0$  is a reference distance within the near-field radius such that  $r_{ex} \geq d_0$ .

The  $\{g_{i,j}\}$  are independent with unit-mean but are not necessarily identically distributed; i.e., the channels from the different  $\{X_i\}$  to  $X_j$  may undergo fading with different distributions. For analytical tractability and close agreement with measured fading statistics, Nakagami fading is assumed, and  $g_{i,j} = a_{i,j}^2$ , where  $a_{i,j}$  is Nakagami with parameter  $m_{i,j}$ . It is assumed that the  $\{g_{i,j}\}$  remain fixed for the duration of a transmission but vary independently from transmission to transmission (block fading).

In the presence of shadowing with a lognormal distribution, the  $\{\xi_{i,j}\}$  are independent zero-mean Gaussian random variables with variance  $\sigma_s^2$ . For ease of exposition, it is assumed that the shadowing variance is the same for the entire network, but the results may be easily generalized to allow for different shadowing variances over parts of the network. In the absence of shadowing,  $\xi_{i,j} = 0$ . While the fading may change from one transmission to the next, the shadowing remains fixed for the entire session.

Each mobile may serve as either a potential relay or a potential source of interference. The *service probability*  $\mu_i$  is defined as the probability that mobile  $X_i$  can serve as a relay along a path from a source to a destination. A Bernoulli variable with probability  $\mu_i$  is used to determine if  $X_i$  is a potential relay, and if it is not, then it is a potential interferer. A mobile may not be able to serve as a relay in a path from  $X_0$  to  $X_{M+1}$  because it is already receiving a transmission, is already serving as a relay in another path, is transmitting, or is otherwise unavailable.

With *interference probability*  $p_i$ , a potentially interfering  $X_i$  transmits in the same time interval as the desired signal. The  $\{p_i\}$  can be used to model the servicing of other streams, controlled silence, or failed link transmissions and the resulting retransmission attempts. The interference transmitted by a potential interferer is independent from one slot to the next; hence, an Aloha medium access control protocol is assumed. Mobiles  $X_0$  and  $X_{M+1}$  do not cause interference, nor do the potential relays. Let  $\mathcal{S}$  denote the indices of the mobiles that actually transmit interference during a time slot. Note that the composition of  $\mathcal{S}$  is fixed for this time slot, but may vary from one slot to the next.

Let  $\mathcal{N}$  denote the noise power. Since the despreading does not significantly affect the desired-signal power, (1) and (2) imply that the instantaneous signal-to-interference-and-noise ratio (SINR) at the mobile  $X_j$  for a desired signal from a relay or source mobile  $X_k$  is

$$\gamma_{k,j} = \frac{g_{k,j}\Omega_{k,j}}{\Gamma^{-1} + \sum_{i \in \mathcal{S}} g_{i,j}\Omega_{i,j}} \quad (3)$$

where

$$\Omega_{i,j} = \begin{cases} 10^{\xi_{k,j}/10} \|X_j - X_k\|^{-\alpha} & i = k \\ \frac{hP_i}{GP_k} 10^{\xi_{i,j}/10} \|X_j - X_i\|^{-\alpha} & i \in \mathcal{S} \end{cases} \quad (4)$$

is the normalized power of  $X_i$  at  $X_j$ , and  $\Gamma = d_0^\alpha P_k / \mathcal{N}$  is the SNR when  $X_k$  is at unit distance from  $X_j$  and fading and shadowing are absent.

The *outage probability* quantifies the likelihood that the interference, shadowing, fading, and noise will be too severe for useful communications. Outage probability is defined with respect to an SINR threshold  $\beta$ , which represents the minimum SINR required for reliable reception. In general, the value of  $\beta$  depends on the choice of coding and modulation. An *outage* occurs when the SINR falls below  $\beta$ . Let  $\Omega_j = \{\Omega_{0,j}, \dots, \Omega_{M,j}\}$  represent the set of normalized powers at  $X_j$ . Conditioning on  $\Omega_j$ , the *outage probability* of the link from  $X_k$  to receiver  $X_j$  is

$$\epsilon_{k,j} = P[\gamma_{k,j} \leq \beta \mid \Omega_j]. \quad (5)$$

The conditioning enables the calculation of the outage probability for every link of any specific or deterministic network geometry, which cannot be done using tools based on stochastic geometry. Restricting the Nakagami parameter  $m_{k,j}$  of the channel between the relay  $X_k$  and receiver  $X_j$  to be integer-valued, the outage probability conditioned on  $\Omega_j$  is found by using deterministic geometry [19] to be

$$\epsilon_{k,j} = 1 - e^{-\beta_{k,j}z} \sum_{s=0}^{m_{k,j}-1} (\beta_{k,j}z)^s \sum_{t=0}^s \frac{z^{-t} H_{t,j}}{(s-t)!} \quad (6)$$

where  $\beta_{k,j} = \beta m_{k,j} / \Omega_{k,j}$ ,  $z = \Gamma^{-1}$ ,

$$H_{t,j} = \sum_{\ell_i \geq 0} \prod_{i \in \mathcal{S}} G_{\ell_i}(i, j) \quad (7)$$

the summation in (7) is over all sets of indices that sum to  $t$ ,

$$G_{\ell}(i, j) = \begin{cases} \Psi_{i,j}^{m_{i,j}} & \ell = 0 \\ \frac{\Gamma(\ell+m_{i,j})}{\ell! \Gamma(m_{i,j})} \left( \frac{\Omega_{i,j}}{m_{i,j}} \right)^\ell \Psi_{i,j}^{m_{i,j}+\ell} & \ell > 0 \end{cases} \quad (8)$$

and

$$\Psi_{i,j} = \left( \beta_{k,j} \frac{\Omega_{i,j}}{m_{i,j}} + 1 \right)^{-1}, \quad i \in \mathcal{S}. \quad (9)$$

## B. Network Simulation

The simulator is organized into four layers, each of which emulates a particular random feature of the network. The layers are implemented as nested *for* loops. The top layer handles the random network topology (i.e., the location of all mobiles in the network), the second layer is concerned with classifying each mobile as either a potential source of interference or a potential relay, the third layer is concerned with determining which of the potential interferers actually transmits (assuming an Aloha protocol with random access probability  $p_i$  is used), while the bottom layer determines which links are actually in an outage. The routing is also handled at the bottom layer.

During each iteration of the top layer, a network topology is generated by placing the locations of the mobiles according to the deterministic geometry model. First the source and destination mobiles are placed in fixed positions, and then one by one, the location of each of the  $M$  remaining mobiles is drawn according to a uniform distribution within the network region. However, if an  $X_i$  falls within the exclusion zone of a previously placed mobile, then it has a new random



location assigned to it as many times as necessary until it falls outside all exclusion zones. This loop is run  $\Upsilon$  times, once per topology.

During each iteration of the second layer, which is run  $K_{t1}$  times, each mobile is independently marked as either being a potential relay (with probability  $\mu_i$ ) or a potential source of interference. Those mobiles that are marked as potential relays cannot transmit interference, and are forced to have transmission probability  $p_i = 0$ .

During each iteration of the third loop, which is run  $K_{t2}$  times, the set of transmitting interferers  $\mathcal{S}$  is found for each time slot, up to some maximum time. Each  $\mathcal{S}$  is found by marking each potential interferer as transmitting by drawing a Bernoulli variable with probability  $p_i$ . Then, for each time slot  $t$ , a matrix is found containing the outage probabilities between all mobiles that may participate in the route (i.e., all mobiles except for the potential interferers).

During each iteration of the bottom layer, which is run  $K_{t3}$  times, each link is marked as either being in an outage or not for each time slot by drawing a Bernoulli variable with probability equal to the corresponding entry in the channel outage matrices. Once the links are marked as being in an outage or not, the set of links that may be used to support a route is identified, and the corresponding routing protocols (described in the next section) may be implemented. Counters are updated to keep track of the key network performance metrics.

### C. Interference Correlation

For a given network topology and service model, there is a common set of mobiles that may produce interference. These mobiles are in locations that are relatively fixed when compared to the timescales of communications. Because of the common randomness in the locations of potentially interfering mobiles, there is correlation in the interference. The correlation is both temporal, because subsequent interfering transmissions come from subsets of the same common set of mobiles, and spatial, due to the common locations of interfering mobiles within a given time slot. The spatio-temporal correlation exists even when the mobiles use Aloha as the MAC protocol, which produces *transmissions* that are locally uncorrelated. While interference correlation is usually neglected, it has become a subject of recent interest [20].

The network model and simulator presented here naturally accounts for interference correlation. This is because during each iteration of the top layer of the simulation, the topology is fixed. Hence, the interfering mobiles selected at the third layer of the simulation is constrained to be drawn from this set. It follows that the calculation of outage probability properly accounts for interference correlation.

Here, the simulator assumes a simple Aloha protocol is used by each potential interferer. We note that other mobiles in the network are likely to be participating in some other, unknown, path. The protocol may be the same or different than the protocol used by the reference path. While it is possible to extend the methodology herein to simulate the separate routing action of neighboring nodes, such an approach is contrary to

the simple simulation advocated by this paper, and requires assumptions to be made about the behavior of the other nodes. In many ad hoc environments, the other nodes may be using completely different routing protocols, may be engaged in direct device-to-device communications, or may be sources of intentional jamming. Rather than trying to simulate the action of each potential interferer, we capture the behavior by appropriately setting the value of the interference probability  $p_i$ . In particular, our investigations have found that for a given routing protocol used by the potential interferers, there will be an equivalent value of  $p_i$  under our model that results in the same performance.

## III. ROUTING MODELS

### A. Routing Protocols

The three routing protocols that are considered are reactive or on-demand protocols that only seek paths from the source to the destination when needed and do not require mobiles to store details about large portions of the network.

The AODV protocol uses an on-demand approach for finding a route during its *path-discovery phase*, which relies on flooding to seek the *fewest-hops path*, which is the path with the smallest number of links or hops. The flooding diffuses request packets simultaneously over multiple routes for the purpose of discovering a successful path to the destination despite link failures along some potential paths. When the first request packet reaches the destination, an acknowledgement is sent back to the source using the fewest-hops path discovered, and each subsequent reception of request packets is ignored. By using this path, the source sends subsequent message packets to the destination during a *message-delivery phase*. This protocol has a very high overhead cost in establishing the fewest-hops path during the path-discovery phase [21], and furthermore the fewest-hops path must be used for message delivery before changes in the channel conditions cause an outage of one or more of its links.

Geographic protocols limit information-sharing costs by minimizing the reliance of mobiles on topology information [2] - [5]. Since geographic routing protocols make routing decisions on a hop-by-hop basis, they do not require a flooding process for path discovery. Two geographic routing protocols are examined: the *greedy forwarding protocol* and the *maximum progress protocol*. Both geographic routing protocols assume that each potential relay knows its physical location and the direction towards the destination.

The greedy forwarding protocol relies on *beacons*, which are periodic brief messages exchanged among mobiles that serve to identify neighboring active mobiles and their locations. Under the greedy forwarding protocol, a source forwards a packet to a relay that is selected from a set of neighboring active mobiles that lie within a *transmission range* of radius  $r_t$ . The next link in the path from source  $X_0$  to destination  $X_{M+1}$  is the link to the relay within the transmission range that shortens the remaining distance to  $X_{M+1}$  the most. There is no path-discovery phase because the relays have the geographic information necessary to route the messages to the destination.

The principal problems with beacons are that they generate additional interference that degrades data packets, and the

location-information may become outdated. With *beaconless routing*, these problems are substantially reduced. Mobiles broadcast short request messages during a path-discovery phase only when they are ready to transmit data packets. The responses to the request messages reveal the identity and location of a neighboring active mobile that is suitable as the next relay during the message-delivery phase.

The maximum progress protocol is a *contention-based* beaconless protocol that comprises alternating *path-discovery phases* and *message-delivery phases*. During a path-discovery phase, a single link to a single relay is discovered. During the following message-delivery phase, a packet is sent to that relay, and then the alternating phases resume until the destination is reached. In a path-discovery phase, the next relay in a path to the destination is dynamically selected at each hop of each packet and depends on the local configuration of available relays. A source or relay broadcasts a *Request-to-Send* (RTS) message to neighboring active mobiles that potentially might serve as the next relay along the path to the destination. The RTS message includes the location of the transmitter. Upon receiving the RTS, a neighboring mobile initiates a timer that has an expiration time proportional to the remaining distance to the destination. When the timer reaches its expiration time, the mobile sends a *Clear-to-Send* (CTS) message as an acknowledgement packet to the transmitter. The earliest arriving CTS message causes the source or previous relay to launch the message-delivery phase by sending the information-bearing message to the mobile that sent that CTS message, and all other candidate mobiles receiving that CTS message cease operation of their timers. The primary advantage of the RTS and CTS messages is that they can be used to establish guard zones surrounding the transmitter and receiver [16]. Potentially interfering mobiles that receive one of these messages within a guard zone are silenced during the acknowledgement and message-delivery phases of the maximum progress protocol. In contrast, while beacons enable direct message transmissions without preliminary RTS/CTS phases, the unsilenced interference may cause outages, thereby significantly degrading the path reliability.

### B. Implementation of Path Selection

A typical network topology of a large network is illustrated in Fig. 1. Each dot represents one of  $M = 200$  mobiles, the five-pointed star at the center of the circle represents the source  $X_0$ , and the six-pointed star on the perimeter represents the destination  $X_{M+1}$ . If a dot is filled, then it may serve as a potential relay. A typical fewest-hops path from  $X_0$  to  $X_{M+1}$  is indicated by the dashed line.

A *candidate link* is a link that does not experience an outage during the path-discovery phase. For AODV, the *candidate paths* from  $X_0$  to  $X_{M+1}$  are paths that can be formed by using candidate links. The candidate path with the fewest hops from  $X_0$  to  $X_{M+1}$  is selected as the *fewest-hops path*. This path is determined by using the *Dijkstra algorithm* [22] with the unit cost of each candidate link. If two or more candidate paths have the fewest hops, the fewest-hops path is randomly selected from among them. If there is no set of

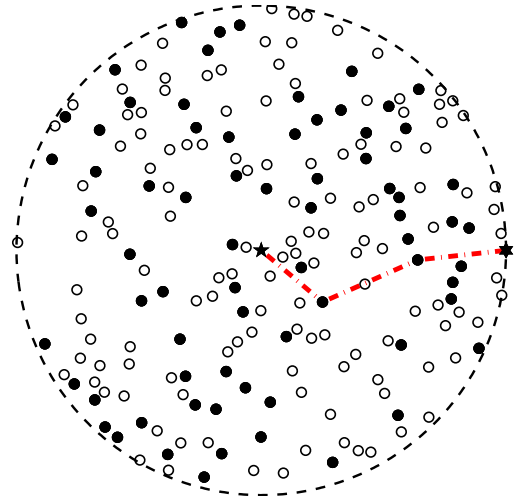


Fig. 1. Typical network topology for two communicating mobiles and  $M = 200$  other mobiles, each of which is represented by a dot. The star at the center of the circle represents the source  $X_0$ , and the star on the perimeter represents the destination  $X_{M+1}$ . If a dot is filled, then it may serve as a potential relay. A typical least-hop path is indicated by the dashed line.

candidate links that allow a path from  $X_0$  to  $X_{M+1}$ , then a *routing failure* occurs and is recorded. If a fewest-hops path exists, then a Monte Carlo simulation is used to determine whether the acknowledgement packet traversing the path in the reverse direction is successful. If it is not or if the message delivery over the fewest-hops path fails, then a routing failure is recorded.

The geographic routing protocols have knowledge of the direction towards the destination, and a *distance criterion* is used to exclude a link from mobile  $X_i$  to mobile  $X_j$  as a link in one of the possible paths from  $X_0$  to  $X_{M+1}$  if  $\|X_j - X_{M+1}\| > \|X_i - X_{M+1}\|$ . These exclusions ensure that each possible path has links that always reduce the remaining distance to the destination. All links connected to mobiles that cannot serve as relays are excluded as links in possible paths from  $X_0$  to  $X_{M+1}$ . Links that have not been excluded are called *eligible links*.

For the greedy-forwarding protocol there is no path-discovery phase, and the eligible links are used to determine the greedy-forwarding path from  $X_0$  to  $X_{M+1}$  during its message-delivery phase. If no path from  $X_0$  to  $X_{M+1}$  can be found or if the message delivery fails, a routing failure is recorded.

A *two-way candidate link* is an eligible link that does not experience an outage in either the forward or the reverse direction during the path-discovery phase. A Monte Carlo simulation is used to determine the two-way candidate links. For the maximum progress protocol, the two-way candidate link starting with source  $X_0$  with a terminating relay that minimizes the remaining distance to destination  $X_{M+1}$  is selected as the first link in the maximum-progress path. The link among the two-way candidate links that minimizes the remaining distance and is connected to the relay at the end of the previously selected link is added successively until the destination  $X_{M+1}$  is reached and hence the maximum-progress path has been determined. After each relay is se-

lected, a message packet is sent in the forward direction to the selected relay. If no maximum-progress path from  $X_0$  to  $X_{M+1}$  can be found or if a message delivery fails, a routing failure is recorded.

Each RTS or CTS message transmitted by the maximum progress protocol during its path-discovery phase establishes a guard zone. If a candidate link exists from the source of an RTS or CTS message to a potentially interfering mobile within the source's guard zone, then that mobile is silenced during the acknowledgement and message-delivery phases. Silencing of a mobile is modeled by removing it from the set  $\mathcal{S}$ . Since the maximum progress protocol is a geographic protocol, potentially interfering mobiles know how far they are from the source of an RTS or CTS message. If they are beyond the guard zone, then they can ignore the message and continue their own transmissions.

In mobile ad hoc networks, the fading processes affecting different links of the same path are not significantly correlated for two reasons. The exclusion zones surrounding the two receivers ensure a significant physical separation. As a result, the two receivers have much different multipath environments and hence experience largely uncorrelated fading. The second reason is that the time between transmissions over successive links in a path usually exceeds the channel coherence time. These two factors decorrelate the fading over different links of the same path.

### C. Performance Metrics

Let  $B$  denote the maximum number of transmission attempts over a link of the path. During the path-discovery phases,  $B = 1$ . During the message-delivery phases,  $B \geq 1$  because message retransmissions over an established link are feasible. For each eligible or candidate link  $l = (i, j)$ , a Bernoulli random variable with failure probability  $\epsilon_l$  is repeatedly drawn until there are either  $B$  failures or success after  $N_l$  transmission attempts, where  $N_l \leq B$ . The *delay of link  $l$*  of the selected path is  $N_l T + (N_l - 1)T_e$ , where  $T$  is the *delay of a transmission over a link*, and  $T_e$  is the *excess delay* caused by a retransmission.

Each network topology  $t$  is used in  $K_t$  simulation trials. The *path delay*  $T_{s,t}$  of a path from  $X_0$  to  $X_{M+1}$  for network topology  $t$  and simulation trial  $s$  is the sum of the link delays in the path during the message-delivery phase:

$$T_{s,t} = \sum_{l \in \mathcal{L}_{s,t}} [N_l T + (N_l - 1)T_e]. \quad (10)$$

where  $\mathcal{L}_{s,t}$  is the set of links constituting the path. If there are  $B$  transmission failures for any link of the selected path, then a routing failure occurs.

If there are  $F_t$  routing failures for topology  $t$  and  $K_t$  simulation trials, then the *probability of end-to-end success* or *path reliability* within topology  $t$  is

$$R_t = 1 - \frac{F_t}{K_t}. \quad (11)$$

Let  $\mathcal{T}_t$  denote the set of  $K_t - F_t$  trials with no routing failures. If the selected path for trial  $s$  has  $h_{s,t}$  links or hops, then

among the set  $\mathcal{T}_t$ , the average conditional *number of hops* from  $X_0$  to  $X_{M+1}$  is

$$H_t = \frac{1}{K_t - F_t} \sum_{s \in \mathcal{T}_t} h_{s,t}. \quad (12)$$

Let  $T_d$  denote the link delay of packets during the path-discovery phase. The average conditional *delay* from  $X_0$  to  $X_{M+1}$  during the combined path-discovery and message-delivery phases is

$$D_t = \frac{1}{K_t - F_t} \sum_{s \in \mathcal{T}_t} (T_{s,t} + 2ch_{s,t}T_d) \quad (13)$$

where  $c = 0$  for the greedy forwarding protocol, and  $c = 1$  for the maximum progress and AODV protocols. Let  $A$  denote the network area and  $\lambda = (M + 1)/A$  denote the density of the possible transmitters in the network. We define the *normalized area spectral efficiency* for the  $K_t$  trials of topology  $t$  as

$$\mathcal{A}_t = \frac{\lambda}{K_t} \sum_{s \in \mathcal{T}_t} \frac{1}{T_{s,t} + 2ch_{s,t}T_d} \quad (14)$$

where the normalization is with respect to the number of message bits transmitted over a successful path. The normalized area spectral efficiency is a measure of the maximum end-to-end throughput in the network. After computing  $R_t$ ,  $D_t$ ,  $H_t$ , and  $\mathcal{A}_t$  for  $\Upsilon$  network topologies, we can average over the topologies to compute the *topological averages*:  $\overline{R}$ ,  $\overline{D}$ ,  $\overline{H}$ , and  $\overline{\mathcal{A}}$ .

The average values of the service probability and the interference probability are defined as

$$\begin{aligned} \overline{\mu} &= \frac{1}{M} \sum_{i=1}^M \mu_i \\ \overline{p} &= \frac{1}{M} \sum_{i=1}^M p_i \end{aligned} \quad (15)$$

respectively. The *relay density*  $\lambda \overline{\mu}$  is a measure of the average number of available relays per unit area. The *contention density*  $\mathbb{E}[\lambda \overline{p}]$  is a measure of the expected number of interfering transmissions per unit area, where the expectation is with respect to the network geometry. When the service probabilities are all the same (i.e.,  $\mu_i = \mu$  for all  $i$ ), and the interference probabilities of the potential interferers are all the same (i.e.,  $p_i = p$  when  $X_i$  is not serving as a potential relay), then the contention density is  $\mathbb{E}[\lambda \overline{p}] = \lambda p(1 - \mu)$ .

## IV. NUMERICAL RESULTS

A host of network topologies and parameter values can be evaluated by the method described in Section II. Here, we consider a representative example that illustrates the tradeoffs among the routing protocols. We consider a network occupying a circular region with normalized radius  $r_{net} = 1$ . The source mobile is placed at the origin, and the destination mobile is placed at distance  $\|X_{M+1} - X_0\|$  from it. Times are normalized by setting  $T = 1$ . Each transmitted power  $P_i$  is equal. There are no retransmissions during the path-discovery phases, whereas no more than  $B$  retransmissions

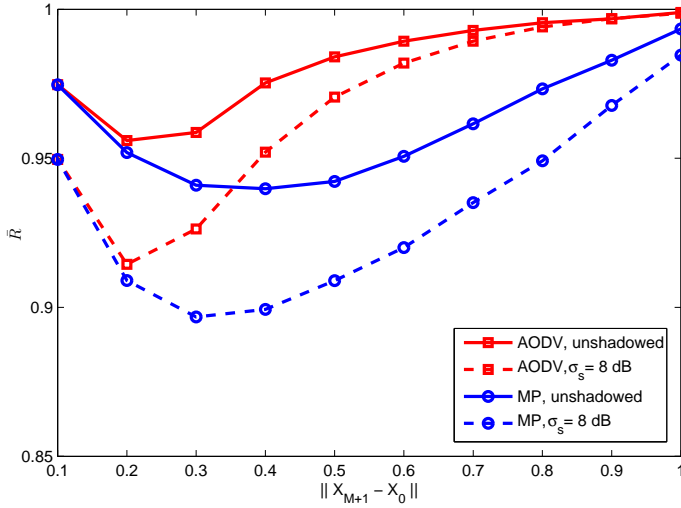


Fig. 2. Average path reliability for request packets of AODV and MP protocols as a function of the distance between source and destination.

are allowed during the message-delivery phases. A *distance-dependent fading* model is assumed, where a signal originating at mobile  $X_i$  arrives at mobile  $X_j$  with a Nakagami fading parameter  $m_{i,j}$  that depends on the distance between the mobiles. We set

$$m_{i,j} = \begin{cases} 3 & \text{if } \|X_j - X_i\| \leq r_f/2 \\ 2 & \text{if } r_f/2 < \|X_j - X_i\| \leq r_f \\ 1 & \text{if } \|X_j - X_i\| > r_f \end{cases} \quad (16)$$

where  $r_f$  is the *line-of-sight radius*. The distance-dependent-fading model characterizes the typical situation in which nearby mobiles most likely are in each other's line-of-sight, while mobiles farther away from each other are not. The severity of the fading decreases, and hence the Nakagami parameter increases, with decreasing distance. The transmission range  $r_t$  defined by the greedy forwarding protocol usually approximates or exceeds  $r_f$ .

The exclusion-zone and guard-zone radii are  $r_{ex} = 0.05$  and  $r_g = 0.15$ , respectively. Other fixed parameter values are  $T_e = 1.2$ ,  $T_d = 0.1$ ,  $M = 200$ ,  $\lambda = 201/\pi$ ,  $\beta = 0$  dB,  $K_t = K_{t1}K_{t2}K_{t3} = 10^6$  ( $K_{t1} = K_{t2} = K_{t3} = 100$ ),  $\Gamma = 0$  dB,  $\alpha = 3.5$ , and  $\Upsilon = 2000$ . The service probabilities are  $\mu_i = \mu$ , whereas the interference probabilities are  $p_i = p$  when  $p_i \neq 0$ . Therefore,  $\lambda\mu$  is the relay density, and  $\mathbb{E}[\lambda\bar{p}] = \lambda p(1 - \mu)$  is the contention density. Unless otherwise stated,  $G/h = 96$ ,  $\alpha = 3.5$ ,  $B = 4$ ,  $r_f = 0.2$ ,  $\mu = 0.4$ , and  $p = 0.3$ . When shadowing is present, it has a lognormal distribution with  $\sigma_s = 8$  dB. However, the transmitted packets encounter the same shadowing in both directions over the same link during both routing phases.

Fig. 2 and Fig. 3 display the average path reliabilities of the request packets and acknowledgement packets, respectively, for the complete selected paths during the path-discovery phases of the AODV and maximum progress (MP) protocols. Fig. 2 depicts the reliabilities both with and without shadowing as a function of the source-destination distance  $\|X_{M+1} - X_0\|$ . Shadowing is assumed in Fig. 3 and all subsequent figures. Fig. 2 shows an initial decrease and then an increase in average

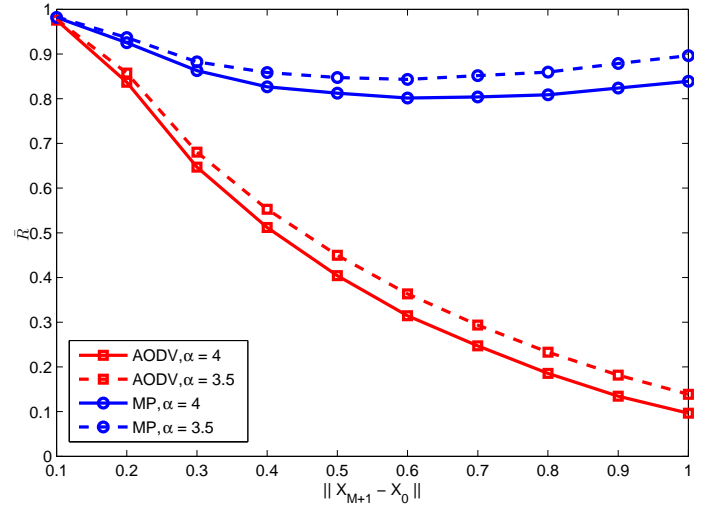


Fig. 3. Average path reliability for acknowledgements of AODV and MP protocols as a function of the distance between source and destination.

path reliability as the source-destination distance increases. This variation occurs because at short distances, there are very few relays that provide forward progress, and often the only candidate or two-way candidate link is the direct link from source to destination. As the distance increases, there are more candidate and two-way candidate links, and hence the network benefits from the diversity. Furthermore, as the destination approaches the edge of the network, the path discovery benefits from a decrease in interference at the relays that are close to the destination. Fig. 2 shows that during the request stage, the AODV protocol provides the better path reliability because it constructs several partial paths before the complete path is determined.

Since the relays are already determined in Fig. 3, the maximum progress protocol shows only a mild improvement with increasing source-destination distance, and this can be attributed almost entirely to the edge effect. It is observed in Fig. 3 that the AODV protocol has a relatively poor path reliability during the acknowledgement stage, which is due to the fact that a specified complete path must be traversed in the reverse direction, where the interference and fading may be much more severe. The maximum progress protocol does not encounter the same problem because the links in its paths are selected one-by-one with the elimination of links that do not provide acknowledgements. Although both the shadowing and the path-loss exponent  $\alpha$  affect both the packets and the interference signals, the two figures indicate that the overall impact of more severe propagation conditions is detrimental for all distances.

Fig. 4 displays the average path reliabilities for the message-delivery phases of the three protocols, assuming that the path-discovery phase, if used, has been successful. The figure illustrates the penalties incurred by the greedy forwarding (GF) protocol because of the absence of a path-discovery phase that eliminates links with excessive shadowing, interference, or fading and creates guard zones for the message-delivery phase. The figure illustrates the role of the transmission range  $r_t$  in determining average path reliability for greedy forwarding



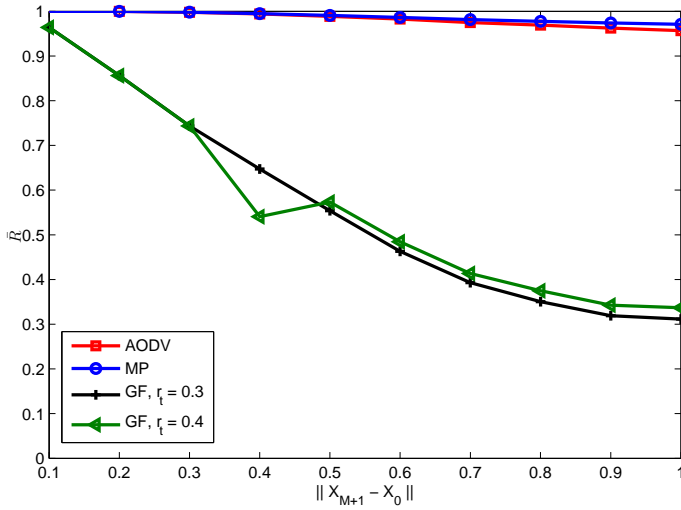


Fig. 4. Average path reliability for message-delivery phase of each routing protocol as a function of the distance between source and destination.

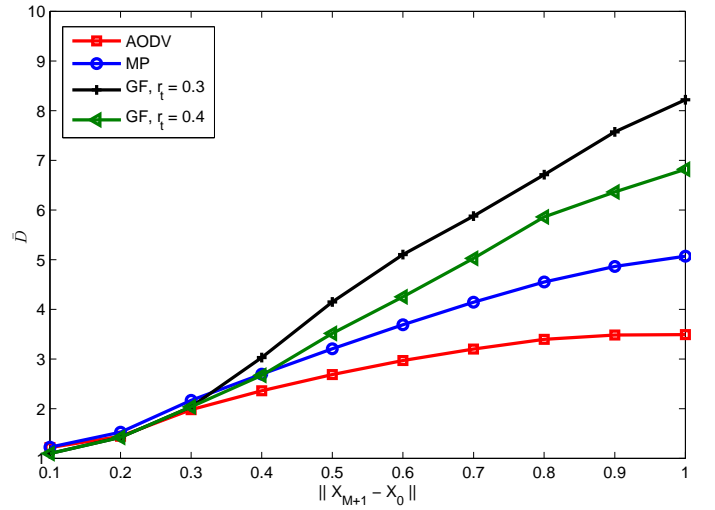


Fig. 6. Average conditional delay of each routing protocol as a function of the distance between source and destination.

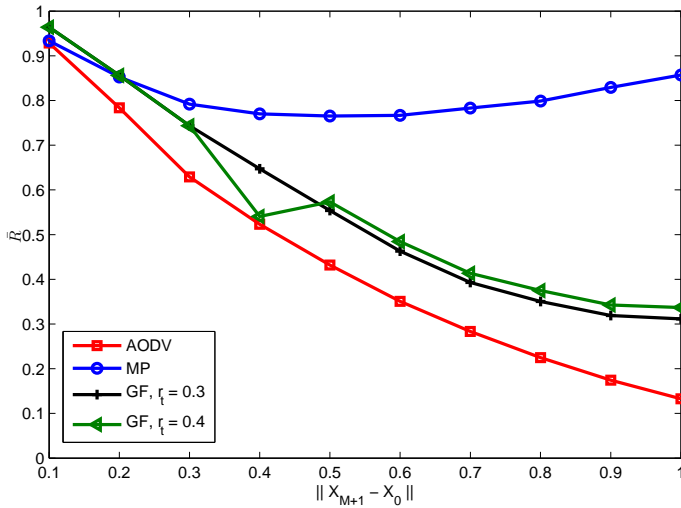


Fig. 5. Average path reliability for both phases of each routing protocol as a function of the distance between source and destination.

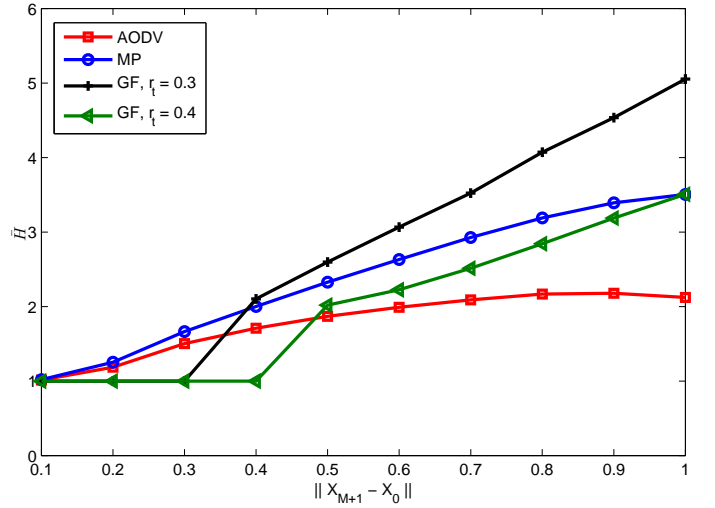


Fig. 7. Average conditional number of hops of each routing protocol as a function of the distance between source and destination.

protocols. As  $r_t$  increases, the links in the complete path are longer and hence less reliable. However, this disadvantage is counterbalanced by the increased number of potential relays and the reduction in the average number of links in a complete path. When  $\|X_{M+1} - X_0\|$  increases slightly above  $r_t$ , there is a sudden jump in the average reliability because the greedy forwarding protocol no longer allows an attempt by the source to directly communicate with the destination in one hop. Instead, two hops over more reliable links must be used.

Fig. 5 shows the overall average path reliabilities for the combined path-discovery and message-delivery phases of all three routing protocols. The AODV protocol is the least reliable. The maximum progress protocol is much more reliable than the greedy forwarding protocol if  $\|X_{M+1} - X_0\|$  is large, but is not as reliable if  $\|X_{M+1} - X_0\| \leq 0.2$  because of the relatively low reliability of its request packets.

The average conditional delay  $\bar{D}$ , the average conditional number of hops  $\bar{H}$ , and the normalized area spectral efficiency  $\bar{A}$  for each routing protocol as a function of  $\|X_{M+1} - X_0\|$  are

displayed in Fig. 6, Fig. 7, and Fig. 8, respectively. The AODV protocol has the smallest  $\bar{D}$ , and if  $\|X_{M+1} - X_0\| \geq 0.5$ , the AODV protocol has the smallest  $\bar{H}$ . The greedy forwarding protocol has the highest  $\bar{A}$  if  $\|X_{M+1} - X_0\|$  is small, whereas the maximum progress protocol has the highest  $\bar{A}$  if  $\|X_{M+1} - X_0\|$  is large. The reason is that the greedy forwarding protocol needs only one hop for a message to reach the destination when  $\|X_{M+1} - X_0\|$  is small, whereas this protocol has reduced reliability and significantly increased average conditional delay when  $\|X_{M+1} - X_0\|$  is large.

The average conditional delay  $\bar{D}$  and the normalized area spectral efficiency  $\bar{A}$  for each routing protocol as a function of the maximum number of retransmissions during the message-delivery phase when  $\|X_{M+1} - X_0\| = 0.5$  are displayed in Fig. 9 and Fig. 10, respectively. The greedy forwarding protocol has a monotonically increasing  $\bar{D}$  and path reliability as  $B$  increases because paths from the source to the destination with longer delays become viable. However, an increase in  $B$  has little effect on  $\bar{D}$  for the AODV and maximum progress



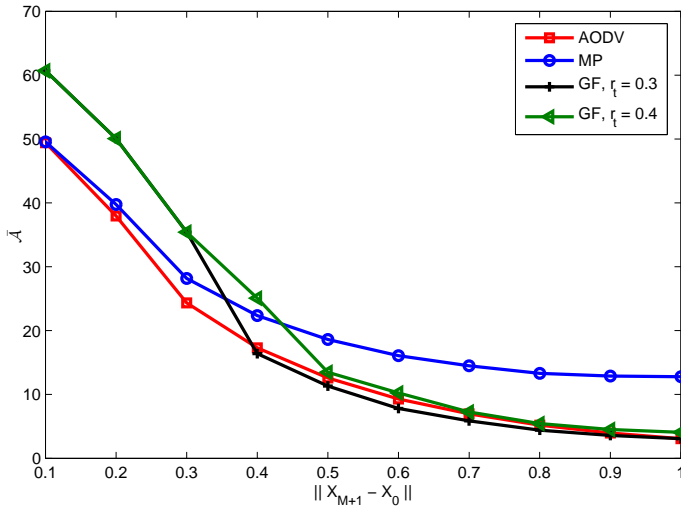


Fig. 8. Area spectral efficiency of each routing protocol as a function of the distance between source and destination.

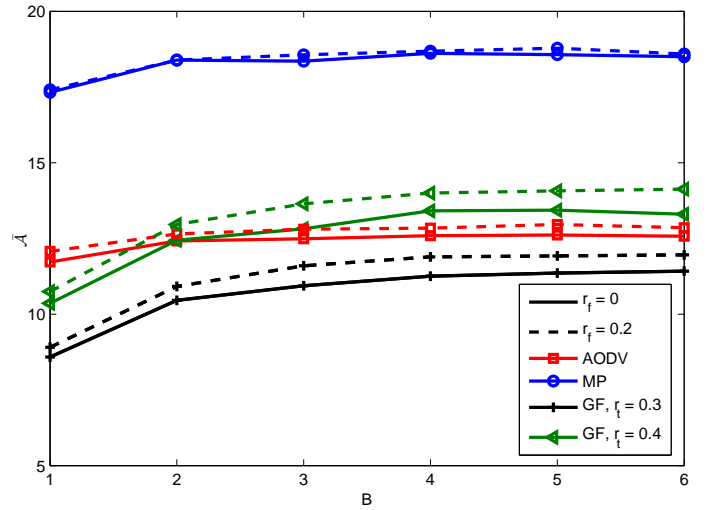


Fig. 10. Normalized area spectral efficiency of each routing protocol as a function of the maximum number of retransmissions during the message-delivery phase when  $\|X_{M+1} - X_0\| = 0.5$ .

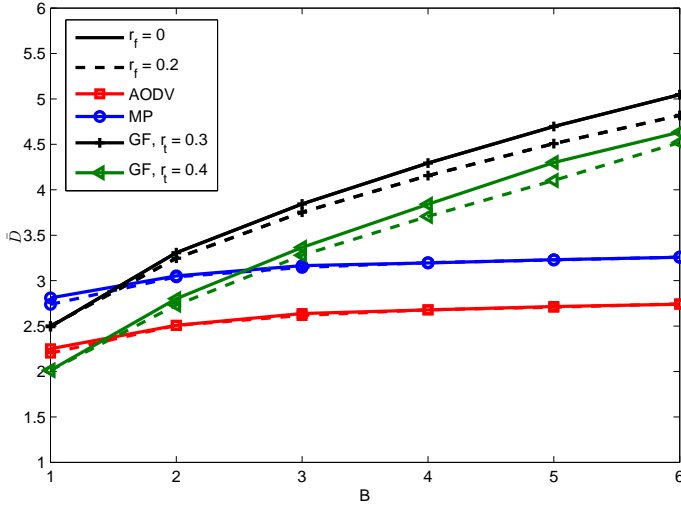


Fig. 9. Average conditional delay of each routing protocol as a function of the maximum number of retransmissions during the message-delivery phase when  $\|X_{M+1} - X_0\| = 0.5$ .

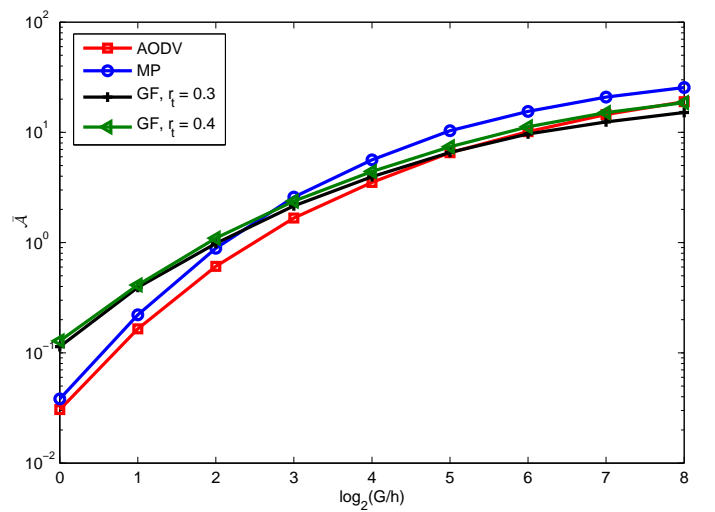


Fig. 11. Area spectral efficiency of each routing protocol as a function of the spreading factor when  $\|X_{M+1} - X_0\| = 0.5$ .

protocols. An increase from  $B = 1$  to  $B = 2$  produces an increase in  $\bar{A}$  for all three protocols, but further increases in  $B$  produce only a minor improvement in  $\bar{A}$ . The reason is that the higher path reliabilities are offset by the increased numbers of successful paths with longer delays. Fig. 9 and Fig. 10 illustrate the losses incurred by the protocols when the fading is the more severe Rayleigh fading ( $r_f = 0$ ) instead of mixed fading with  $r_f = 0.2$ . In all other figures,  $r_f = 0.2$ .

The critical role of the spreading factor  $G$  in suppressing interference is illustrated in Fig. 11 for  $\|X_{M+1} - X_0\| = 0.5$ . The normalized area spectral efficiency  $\bar{A}$  of each protocol increases monotonically with  $G/h$ , but the rate of increase is greatest for the maximum progress protocol. When the distance is  $\|X_{M+1} - X_0\| = 0.5$ , the maximum progress protocol provides the largest  $\bar{A}$  if  $G/h \geq 8$ . In the absence of spreading, the greedy forwarding protocol provides the largest  $\bar{A}$ .

Fig. 12 and Fig. 13 illustrate the average path reliability and the area spectral efficiency, respectively, for each routing protocol when  $\|X_{M+1} - X_0\| = 0.5$  as a function of the contention density  $\mathbb{E}[\lambda\bar{p}]$  with the relay density  $\lambda\mu$  as a parameter. The figures indicate the degree to which an increase in the contention density is mitigated by an increase in the relay density. The figures were generated by varying  $p$  and  $\mu$  while maintaining  $M = 200$  and  $\lambda = 201/\pi$ . However, nearly the same plots are obtained by varying  $M$  or  $\lambda$  while maintaining  $p = 0.3$  and  $\mu = 0.4$ . Thus, the contention density and relay density are of primary importance, not the individual factors  $p$ ,  $\mu$ , and  $\lambda$ .

The figures can be used to determine which protocols are suitable for achieving the performance requirements. For example, if the average path reliability is required to be 0.9 when  $\|X_{M+1} - X_0\| = 0.5$ , then Fig. 12 indicates that the maximum progress protocol or greedy forwarding protocol is

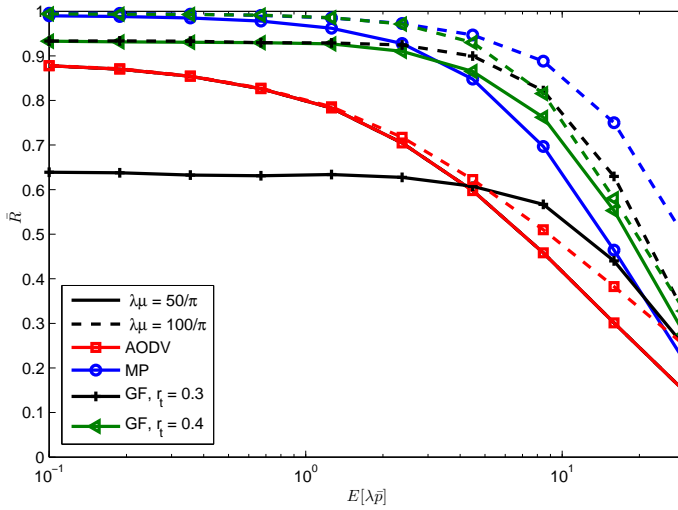


Fig. 12. Average path reliability for each routing protocol when  $\|X_{M+1} - X_0\| = 0.5$  as a function of the contention density with the relay density as a parameter.

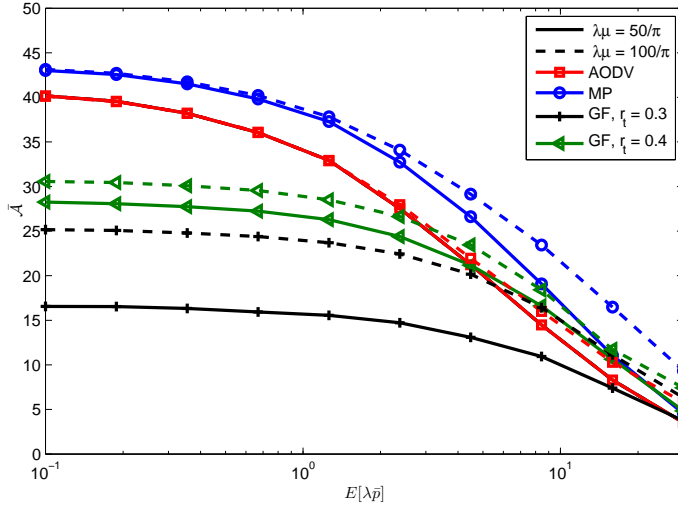


Fig. 13. Area spectral efficiency for each routing protocol when  $\|X_{M+1} - X_0\| = 0.5$  as a function of the contention density with the relay density as a parameter.

necessary. If in addition the relay density is  $\lambda\mu = 50/\pi$ , then the maximum progress protocol and the greedy forwarding protocol with  $r_t = 0.4$  meet the requirement, and  $\mathbb{E}[\lambda\bar{p}] \leq 1$  can be accommodated.

For both values of the relay density, the AODV protocol exhibits a lower average path reliability and area spectral efficiency than the maximum progress protocol. The greedy forwarding protocol with  $r_t = 0.3$  has a poor average path reliability and area spectral efficiency when the relay density is low because of the paucity of potential relays within its transmission range. When  $r_t = 0.4$  and both the relay density and contention density are large, the greedy forwarding provides an area spectral efficiency superior to that of the AODV protocol and approaching that of the maximum progress protocol.

## V. CONCLUSIONS

This paper presents performance evaluations and comparisons of two geographic routing protocols and the popular AODV protocol. The general methodology of this paper can be used to provide a significantly improved analysis of multihop routing protocols in ad hoc networks. Many unrealistic and improbable assumptions and restrictions of existing analyses can be discarded.

The tradeoffs among the average path reliabilities, average conditional delays, average conditional numbers of hops, and area spectral efficiencies and the effects of various parameters have been shown for a typical ad hoc network. Since acknowledgements are often lost due to the nonreciprocal interference on the reverse paths, the AODV protocol has a relatively low path reliability, and its implementation is costly because it requires a flooding process. In terms of the examined performance measures, the greedy forwarding protocol is advantageous when the separation between the source and destination is small and the spreading factor is large, provided that the transmission range and the relay density are adequate. The maximum progress protocol is more resilient when the relay density is low and is advantageous when the separation between the source and destination is large.

The approach presented in this paper can be readily extended to cover more sophisticated network models. For instance, by incorporating a discrete-time mobility model, systems with high mobility and carry-store-and-forward networks can be accommodated. While the focus has been on unicast networks, the extension to multicast is straightforward.

## REFERENCES

- [1] C. E. Perkins and E. M. Royer, "Ad hoc on demand distance vector routing", *Proc. IEEE MOBICom*, pp. 90-100, 1999.
- [2] F. Cadger, K. Curran, J. Santos, and S. Moffett, "A survey of geographical routing in wireless ad-hoc networks," *IEEE Commun. Surveys Tuts.*, vol. 15, pp. 621-653, 2nd quarter, 2013.
- [3] C. Petrioli, M. Nati, P. Casari, M. Zorzi, and S. Basagni, "ALBA-R: Load-balancing geographic routing around connectivity holes in wireless sensor networks," *IEEE Trans. Parallel and Distrib. Syst.*, vol. 25, pp. 529-539, March 2014.
- [4] S. Ruhup and I. Stojmenovic, "Optimizing communication overhead while reducing path length in beaconless georouting with guaranteed delivery for wireless sensor networks," *IEEE Trans. Computers*, vol. 62, Dec. 2013.
- [5] K. Z. Ghafoor et al., "Intelligent beaconless geographical forwarding for urban vehicular environments," *Wireless Networks*, vol. 19, pp. 345-362, April 2013.
- [6] A. Zanella, A. Bazzi, G. Pasolini, and B. M. Masini, "On the impact of routing strategies on the interference of ad hoc wireless networks," *IEEE Trans. Commun.*, vol. 61, pp. 4322-4333, Oct. 2013.
- [7] I. Byun, J. G. Andrews, and K. S. Kim, "Delay-constrained random access transport capacity," *IEEE Trans. Wireless Commun.*, vol. 12, pp. 1628-1639, April 2013.
- [8] Y. Chen and J. G. Andrews, "An upper bound on multihop transmission capacity with dynamic routing selection," *IEEE Trans. Inform. Theory*, vol. 58, pp. 3751-3765, June 2012.
- [9] P. H. J. Nardelli, M. Kaynia, P. Cardieri, and M. Latva-aho, "Optimal transmission capacity of ad hoc networks with packet retransmissions," *IEEE Trans. Wireless Commun.*, vol. 11, pp. 2760-2766, Aug. 2012.
- [10] P. H. J. Nardelli, P. Cardieri, and M. Latva-aho, "Efficiency of wireless networks under different hopping strategies," *IEEE Trans. Wireless Commun.*, vol. 11, pp. 15-20, Jan. 2012.
- [11] R. Vaze, "Throughput-delay-reliability tradeoff with ARQ in wireless ad hoc networks," *IEEE Trans. Wireless Commun.*, vol. 10, pp. 2142-2149, July 2011.

- [12] J. G. Andrews, S. Weber, M. Kountouris, and M. Haenggi, "Random access transport capacity," *IEEE Trans. Wireless Commun.*, vol. 9, pp. 2101-2111, June 2010.
- [13] H. ElSawy, E. Hossain, and M. Haenggi, "Stochastic geometry for modeling, analysis, and design of multi-tier and cognitive cellular wireless networks: a survey," *IEEE Commun. Surveys Tut.*, vol. 15, pp. 996-1019, 3rd quarter, 2013.
- [14] M. Haenggi, *Stochastic Geometry for Wireless Networks*. Cambridge University Press, 2012.
- [15] S. N. Chiu, D. Stoyan, W. S. Kendall, and J. Mecke, *Stochastic Geometry and its Applications*, 3rd ed., Wiley, 2013.
- [16] D. Torrieri and M. C. Valenti, "Exclusion and guard zones in DS-CDMA ad hoc networks," *IEEE Trans. Commun.*, vol. 61, pp. 2468-2476, June 2013.
- [17] D. Torrieri, S. Talarico, and M. C. Valenti, "Multihop routing in ad hoc networks," *Proc. IEEE Military Commun. Conf. (MILCOM)*, (San Diego, CA), Nov. 2013.
- [18] D. Torrieri, S. Talarico, and M. C. Valenti, "Performance analysis of geographic routing protocols in ad hoc networks," *Proc. IEEE Military Commun. Conf. (MILCOM)*, (Baltimore, MD), Oct. 2014.
- [19] D. Torrieri and M. C. Valenti, "The outage probability of a finite ad hoc network in Nakagami fading," *IEEE Trans. Commun.*, vol. 60, pp. 3509-3518, Nov. 2012.
- [20] R. K. Ganti, and M. Haenggi, "Spatial and temporal correlation of the interference in ALOHA ad hoc networks," *IEEE Commun. Letters*, vol. 13, pp. 631-633, Sep. 2009.
- [21] I. S. Haque, "On the overheads of ad hoc routing schemes," *IEEE Systems J.*, vol. 9, pp. 605-614, June 2015.
- [22] R. A. Brualdi, *Introductory Combinatorics*, 5th ed., Pearson Prentice Hall, 2010.



**Don Torrieri** is a research engineer and Fellow of the US Army Research Laboratory. His primary research interests are communication systems, adaptive arrays, and signal processing. He received the B. S. degree from the Massachusetts Institute of Technology and the M. S. and Ph.D. degrees from the University of Maryland. He is the author of many articles and several books including *Principles of Spread-Spectrum Communication Systems*, third ed. (Springer, 2015). He has taught many graduate courses at Johns Hopkins University and many short

courses. In 2004, he received the IEEE Military Communications Conference Achievement award for sustained contributions to the field. In 2014, he received the Army Research Laboratory Publication Award.



**Salvatore Talarico** received the B.Sc and M.Sc. degrees in electrical engineering from University of Pisa, Pisa, Italy in 2006 and 2007 respectively, and the Ph.D in electrical engineering from West Virginia University, Morgantown, WV in 2015. From 2008 until 2010, before joining West Virginia University, he worked in the R&D department of Screen Service Broadcasting Technologies (SSBT) as an RF System Engineer. His research interests lies in the area of software defined radio, information theory, and wireless communications.



**Matthew C. Valenti** is a Professor in the Lane Department of Computer Science and Electrical Engineering at West Virginia University and site director for the Center for Identification Technology Research (CITeR), an NSF Industry/University Co-operative Research Center (IUCRC). His research is in the area of wireless communications, including cellular networks, military communication systems, sensor networks, and coded modulation for satellite communications. He is active in the organization of major conferences, including serving as the Technical Program Vice Chair for MILCOM 2015 and Globecom 2013, and as a track or symposium chair for MILCOM ('10,'12,'14), ICC ('09,'11), Globecom ('15), and VTC ('07). He is an Executive Editor for IEEE Transactions on Wireless Communications, an Editor for IEEE Transactions on Communications, and the Chair of ComSoc's Communication Theory Technical Committee. Dr. Valenti is an alumnus of Virginia Tech, having received his BSEE in 1992 and Ph.D. in 1999, under the support of the Bradley Fellowship. In addition, he received a MSEE from Johns Hopkins and worked as an Electronics Engineer at the US Naval Research Laboratory. He is registered as a Professional Engineer in the state of West Virginia.